

UCLA

UCLA Previously Published Works

Title

Effects of Thoracic Pressure Changes on MRI Signals in the Brain

Permalink

<https://escholarship.org/uc/item/75t6v3r0>

Journal

Cerebrovascular and Brain Metabolism Reviews, 35(6)

ISSN

1040-8827

Authors

Wu, Paula
Bandettini, Peter A
Harper, Ronald M
[et al.](#)

Publication Date

2015-06-01

DOI

10.1038/jcbfm.2015.20

Peer reviewed

ORIGINAL ARTICLE

Effects of thoracic pressure changes on MRI signals in the brain

Paula Wu¹, Peter A Bandettini^{1,2}, Ronald M Harper^{3,4} and Daniel A Handwerker¹

Cerebrovascular stressors, such as breath holding or CO₂ inhalation, cause global magnetic resonance imaging (MRI) signal changes. In this study, we show that intrathoracic pressure changes cause rapid MRI signal alterations that have similar spatial patterns to the changes associated with breath holding or CO₂ inhalation. Nine subjects performed the Valsalva maneuver during functional MRI data collection. Expiratory pressures ranged from 10 to 40 mm Hg. Breath holds ending on either inhalation or exhalation were also collected. The maximal and minimal functional MRI (fMRI) signal scaled with thoracic pressure load, and the overall amplitude of responses to the Valsalva varied, depending on brain tissue. Additionally, a Valsalva effort as short as 5 seconds yielded signal changes similar in spatial distribution and magnitude to a 20-second breath hold, suggesting potential applications of the Valsalva maneuver for calibrated fMRI experiments.

Journal of Cerebral Blood Flow & Metabolism (2015) **35**, 1024–1032; doi:10.1038/jcbfm.2015.20; published online 25 February 2015

Keywords: breath hold; cerebral blood flow; functional MRI; hypercapnia; Valsalva

INTRODUCTION

Cerebrovascular responses to global stresses have long been used to better understand brain function and disease, and to study the tools used to measure brain activity. These global stressors include injecting acetazolamide, ingesting caffeine, breathing CO₂- or O₂-enriched or impoverished air, and breath holding.^{1–4} In this study, we quantify an additional stressor. We show that changes in intrathoracic chest pressure via the Valsalva maneuver globally and parametrically modulate functional magnetic resonance imaging (fMRI) response magnitudes. This task varies intrathoracic pressure in a manner that is noninvasive, low risk, and intuitively simple to perform. As such, the quantification of the pressure effects, presented here, adds to the ways researchers and clinicians can alter and study cerebrovascular responses.

The effects of changes in intrathoracic pressure on blood flow have long been known. The Valsalva maneuver is a standard clinical tool that consists of an exhalation against a closed glottis or another closed system, with the goal of increasing intrathoracic pressure to 20 to 40 mm Hg. The maneuver involves increasing intrathoracic pressure during a breath hold, and elicits consistent autonomic responses including heart rate, blood pressure, and blood flow changes.⁵ The effects of intrathoracic pressure changes on cerebral blood flow have been less studied. Invasive internal carotid artery and Transcranial Doppler measurements have shown that the Valsalva maneuver elicits consistent cerebral blood flow responses.^{6–8} One limitation of these studies is that they use a single intrathoracic pressure target, making it impossible to distinguish the effect of hypercapnia during the Valsalva breath hold from the effect of the pressure changes. One fMRI study has shown that controlling for chest circumference—a proxy for chest pressure—during a breath

hold reduces variability of the blood oxygenation level-dependent (BOLD) response.⁹ Others have shown that flow changes in the middle cerebral artery using transcranial Doppler are more predictable when blood pressure changes are also modeled.¹⁰ We hypothesized that changes in pressure, even with a constant breath hold duration, would modulate the fMRI response.

We compared the fMRI responses to a breath hold with those induced by Valsalva maneuvers involving different levels of intrathoracic pressure and breath hold duration. We compared magnitudes and dynamics, as well as the spatial pattern of the maps to determine whether the signal changes corresponded to those of the other global stresses.

We found that the Valsalva maneuver can reliably modulate the MRI signal based on thoracic pressure with a similar spatiotemporal MRI response to breath holding without pressure feedback. The mechanisms for these signal changes are an area of future investigation, as they may reflect rapid changes in blood volume and blood flow with alterations in intrathoracic pressure. Here, we report these findings, and discuss their potential utility for fMRI calibration and for vascular patency assessment.

MATERIALS AND METHODS

Subjects and Imaging Parameters

Nine healthy subjects (5 male, age 29 ± 8 years) participated after granting informed consent under an NIH Combined Neuroscience Institutional Review Board-approved protocol (93-M-0170) in accordance with the Belmont Report and US Federal Regulations that protect human subjects. Data were collected in a GE 3 T HDx scanner (Waukesha, WI, USA) with a 16-channel head coil using a GRE EPI sequence. Eight oblique slices were collected at a resolution of 3.75 × 3.75 × 4 mm³ (repetition time = 400 ms,

¹Section on Functional Imaging Methods, Laboratory of Brain and Cognition, National Institute of Mental Health, Bethesda, Maryland, USA; ²Functional MRI Facility, National Institute of Mental Health, Bethesda, Maryland, USA; ³Department of Neurobiology, David Geffen School of Medicine, University of California at Los Angeles, Los Angeles, California, USA and ⁴Brain Research Institute, University of California at Los Angeles, Los Angeles, California, USA. Correspondence: DA Handwerker, Section on Functional Imaging Methods, Laboratory of Brain and Cognition, National Institute of Mental Health, 10 Center Drive, Room 1D80, MSC1148, Bethesda, MD 20814, USA. E-mail: handwerkerd@mail.nih.gov

This research was supported by the NIMH Intramural Research Program at NIH: ZIAMH002783. The study was approved under NIH Combined Neuroscience Institutional Review Board protocol #93-M-0170 (ClinicalTrials.gov identifier: NCT00001360).

Received 22 April 2014; revised 11 December 2014; accepted 9 January 2015; published online 25 February 2015

echo time=30 ms, flip angle=30, parallel imaging method: ASSET; acceleration factor: 2). T1-weighted MPRAGE images ($0.86 \times 0.86 \times 1.2 \text{ mm}^3$ voxels) were also collected for anatomic registration.

Breath Hold and Valsalva Challenges

Valsalva task setup. Each subject performed the Valsalva maneuver at varying durations and pressures by forcibly exhaling into a custom-built mechanism that provided real-time feedback regarding pressure. Subjects exhaled into an apparatus consisting of a noncompliant tube (polyethylene tubing, 1/16" internal diameter), connected to a Honeywell 142PC05G pressure sensor (Freeport, IL, USA) outside the MRI scanner room. The transducer interfaced with a computer using a National Instruments analog-to-digital converter (Austin, TX, USA). During breathing challenges, a visual display changed from red to green when the target pressure range was reached (-2 to $+5 \text{ mmHg}$ of the target pressure), and a scale continuously displayed the pressure attained in the tube. Stimulus presentation and pressure data recordings were implemented in LabVIEW (www.ni.com/labview). In addition to the pressure data, task compliance was monitored using a pneumatic belt around the chest to measure relative thoracic circumference, and a pulse oximeter on a finger was used to record the heartbeat.

Pressure trials. Volunteers performed the Valsalva maneuver at varying pressures and constant duration. At each pressure level, five total Valsalva holds were performed, and each Valsalva hold began and ended with a paced breathing period. During hold periods, subjects held their breath for 20 seconds while exhaling into the tube to maintain a pressure of 10, 20, 30, or 40 mm Hg after inhalation. During the breathing periods before and after hold periods, subjects received instructions to breathe in and out at 1/6 Hz for 39 seconds, starting and ending on inspiration. Instructed pacing of the breathing cycle helped subjects enter the Valsalva hold more calmly, and with less head motion. Each breathing challenge run lasted 334 seconds (835 fMRI volumes). The first 29.2 seconds (73 fMRI volumes) of the first paced-breathing period of each pressure challenge were excluded from all analyses so that the volunteers' MRI signal changes represented a steady breathing rate. Each of the five trials included 146 volumes (58.4 seconds).

Duration trials. To isolate the effect of breath hold duration, the Valsalva maneuver was also performed at varying durations at a constant pressure of 30 mm Hg. As with pressure runs, each run included five breathing challenges that began and ended with a 39-second paced-breathing period. Hold durations lasted for 5, 10, 15, or 25 seconds. Responses during these durations were compared against the 20-second trial collected at 30 mm Hg described earlier.

Breath hold only. Volunteers were also asked to perform the breath hold with no pressure feedback. Breath holds were performed after a final exhalation, as well as after a final inhalation. For the breath hold after exhalation, a 3-second exhalation preceded a 17-second breath hold, so that the total time between inhalation of air was 20 seconds. Breath hold, duration, and pressure runs were randomized for each subject. When describing results, the breath hold trials without pressure feedback are called 'breath hold,' and the breath hold trials with pressure feedback are called 'Valsalva'.

Data Analysis

Preprocessing. The echo planar imaging (EPI) time series data were corrected for head motion via a rigid-body volume registration, time shifted to align slices in each volume to the same temporal origin, and converted to percent change from the mean. Low frequency drifts were removed using 0 to 3rd order polynomials. For each condition, the MRI time series were averaged across the five trials, starting 9.8 seconds before the hold period. Signal change maps were calculated for each breathing challenge within the regions-of-interest (ROIs) of each tissue type. The trial-averaged data were temporally smoothed (0.5 Hz low-pass filter) to increase the temporal signal-to-noise ratio and to decrease the effect of fluctuations that are faster than hemodynamic responses on estimates of response timing and magnitudes. AFNI (<http://afni.nimh.nih.gov>), an open source software package for the analysis and display of functional MRI data, was used for image processing and brain image visualization.¹¹

Regions of interest. Region-of-interest maps were created from the T1-weighted anatomic images using Freesurfer (<http://surfer.nmr.mgh.har>

[vard.edu](http://surfer.nmr.mgh.harvard.edu))¹² to produce masks for cortical gray matter, subcortical gray matter, white matter, and cerebral spinal fluid (ventricles) areas. The T1-weighted anatomic images were registered to the EPI data using a 12-parameter affine transformation. The tissue ROI masks were transformed and down-sampled to the voxel resolution of the EPI data. To account for partial volume effects and potential misregistration due to spatial distortion in the EPI images, voxels that included more than 25% of two types of tissue were excluded from analysis. The cortical gray, subcortical gray, white, and cerebrospinal fluid (CSF) masks across volunteers had a range of 2,413 to 3,884, 165 to 775, 3,857 to 4,905, and 94 to 759 voxels ($3.75 \times 3.75 \times 4 \text{ mm}^3$), respectively.

Region-of-interest analyses were conducted in native spatial orientation and resolution. Some analyses averaged measures across the population. For these analyses, the T1-weighted anatomic images were aligned to a common space that was mapped to the Talairach-Tournoux atlas. All values were calculated in native spatial orientation and then warped to the common space.

Data analysis. The global fMRI response to the Valsalva included a decline below baseline during the Valsalva-hold period (response valley), followed by an increase above baseline soon after the end of the hold (response peak). The minimal response during valleys and the maximal response during peaks were calculated on a voxel-wise basis. For 20-second breathing challenges, the valley response was defined as the minimum response magnitude in the first 15 seconds of the breath hold onset, and the maximum amplitude between 5 and 39 seconds after the hold onset was selected as the peak signal response. These windows were adjusted accordingly for longer and shorter duration trials. Valley and peak response magnitudes were calculated as the difference between maximal or minimal response amplitudes and the magnitude during the 13-second breathing period before the hold period or the baseline period. For ROI analyses, response magnitudes and timings were calculated using the average time series for all voxels within each ROI. In addition, the slopes of peak and valley magnitude changes versus chest pressure were also calculated, using linear regression. These slopes were calculated on a voxelwise basis for the whole brain, or within the average signal in an ROI.

Heart rate calculations. Heart rate was calculated as the inverse of time between arterial oxygen saturation (SaO_2) peaks from pulse oximeter traces using a custom MATLAB script. Since hand movement and other factors added noise in automatic peak detection, detected peaks were manually examined and edited to confirm accuracy. If a few-second span was too noisy to clearly detect peaks, then peak locations were estimated based on neighboring peak spacing. To decrease the potential of experimenter bias, the review and editing processes were blinded to task condition for each time course, and without checks whether errors occurred during breathing or hold periods.

Under normal conditions, the typical pulse oximeter heart beat trace included a peak in SaO_2 during left ventricular systolic ejection, followed by the dicrotic notch, and a dip in SaO_2 caused by the closure of the aortic valve. A second peak then occurs in SaO_2 after the dicrotic notch.¹³ In some volunteers, peaks after the dicrotic notch were falsely labeled as 'true' heart beats when the heart rate increased and ventricular systolic ejection volume probably decreased during the Valsalva challenge. Manual edits were able to accurately distinguish true SaO_2 peaks.

RESULTS

Task Compliance

Almost all subjects successfully completed the tasks (Figures 2A, 2B, 2H, and 2I). One subject was unable to maintain the target pressure during the 40 mm Hg 20-second run and the 30 mm Hg 25-second run. Another subject failed to reach 30 mm Hg for one of five 10-second duration trials. Based on the respiratory belt data, five subjects may have taken a breath during 1 to 3 trials of the 40 total trials, with no more than one possible breath during each task condition. Head motion was calculated as the Euclidian norm of the six motion parameters. The maximum head motion in any single run in any subject was only 1.8 mm. In some subjects, there was a slight trend toward increased head motion with increasing pressure, but this was small, and not consistent across the group.

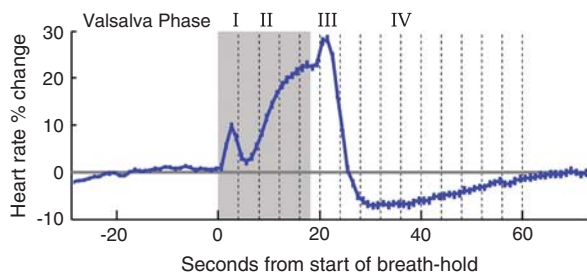


Figure 1. Heart rate changes during the four phases of the Valsalva maneuver. Mean and standard deviation of 4 Valsalva maneuvers across 57 volunteers. The gray-shaded area marks the breath holding period. These data were collected as part of another study, and the figure is adapted from a previously published figure.²⁶

Heart Rate Changes During the Valsalva Maneuver

Figure 1 shows the heart rate changes during different phases of the Valsalva. The Valsalva maneuver elicited a rise in heart rate during phase II (which is the phase during the breath hold), a peak rate in phase III (upon release), and a subsequent return to baseline in Valsalva phase IV.⁵ Mean heart rates across volunteers showed the expected standard four-phase Valsalva autonomic response⁵ during the 20-, 30-, and 40-mm Hg challenges (Figure 2C) and during the 5- to 25-second duration challenges at 30 mm Hg (Figure 2J). Individual subject heart rate responses largely showed similar Valsalva phases as the group mean, but 3 to 4 subjects did not show Valsalva phase-induced heart rate changes in the 5-second duration and the 20 mm Hg runs, respectively. While the mean breath hold after exhalation trials revealed a short heart rate increase after the challenge (phase III), heart rate did not increase during the breath hold (phase II).

Thoracic Pressure Increases Correlated with Increases in Magnetic Resonance Imaging Signal Amplitude

The MRI signal response to the Valsalva was characterized by an initial decline, followed by a rise (Figures 2D–2G and 2K–2N). Across subjects, in all tissues and hold trials, average responses reached a valley 10 to 11 seconds after the start of the hold, and then rose to reach a maximum 7 to 9 seconds after the breath hold period ended.

The signal changes in gray matter, white matter, and CSF were correlated with load pressure. ($P < 0.001$; Figure 2, Figures 3A–3D). The magnitude of response minima also scaled with thoracic pressure (Figures 3E–3H).

To disambiguate the effects of hypercapnia and intrathoracic pressure on the response, we subtracted the response for breath hold initiation-on-exhalation from the responses to all other hold trials. Here, we assumed that a breath hold initiating on exhalation resulted in a comparably minimal increase in thoracic pressure, thus having none of the blood pressure and flow changes associated with increased thoracic pressure. The hold-on-exhale has a very small undershoot during the hold, and the signal peak after the hold termination has a similar peak magnitude to the hold-on-inhale and 10 mm Hg breath hold responses (Figures 2D–2G).

The group-averaged responses are shown in the insets of Figures 2D–2G. The solid black lines in Figure 3 show the linear regression fits across subjects before subtracting the ‘hold-on-exhalation,’ or non-Valsalva-time series. The dashed black lines show the fit after subtraction. Subtracting the hold-on-exhale response for each subject did not alter the average slope between intrathoracic pressure and MRI signal magnitude. The intercept moved closer to zero, particularly for gray and subcortical gray-matter voxels (Figures 3A and 3D). An intercept that is close to

zero after removing hold-on-exhalation values implies that the 10 mm Hg response across subjects has a similar magnitude to the hold-on-exhalation trials. The subtraction changed the r^2 fits to the peak magnitudes by less than 0.02, and did not alter statistical significance (Figures 3A–3D). After subtraction, the fits to the valley magnitudes had lower r^2 values, and the P values for gray matter, subcortical gray matter, and CSF are no longer significant ($P < 0.05$ Bonferroni, correcting for eight regressions). The intercepts were also similar, implying that subtracting the hold-on-exhalation response did not significantly alter the valley magnitudes (Figures 3E–3H).

Breath Hold Duration and Magnetic Resonance Imaging Signal Changes

When the duration of breath holds with a 30 mm Hg intrathoracic pressure was increased from 5 to 25 seconds, the average MRI signal response showed a consistent MRI signal undershoot during the hold and an increase above baseline after release (Figures 2K–2N). The relationship between hold duration and the maximum or minimum MRI signal magnitudes was assessed. Maximal MRI signal amplitudes increased with hold duration in gray matter ($P < 0.001$), and white matter ROIs ($P = 0.002$); no relationship appeared between the minimal magnitude and hold duration in any tissue type.

The relationship between hold duration and the time-to-MRI signal maxima or minima was also assessed (Table 1). The time-to-peaks from the end of the breath holds decreased with increasing hold duration in all tissues ($P < 0.006$). For example, the mean time-to-peak line is 8.6 seconds for a 5-second duration hold, and 6.9 seconds for a 25-second duration hold. The time-to-valley did not vary with hold duration across trials, with one exception. The 5-second hold showed a significantly earlier time-to-valley in the gray- and white-matter ROIs, compared with the 10-second hold ($P < 0.001$), because the fMRI signal was still on its initial downward descent upon breath release.

Spatial Distribution of Signal Changes Due to Pressure

Magnetic resonance imaging signal valley and peak magnitudes across brain areas and load pressures were examined. Figure 4 shows a slice for several types of trials from a single subject. With the same intensity scaling across metrics (Figure 4B), it is clear that voxel-wise responses get larger in gray matter and CSF as chest pressure increases.

While Figure 4B shows voxelwise response magnitudes increasing with pressure in a single subject, Figure 5 shows this outcome across the population. We calculated, on a voxel-wise basis, the slope of the signal change versus load pressure. The resulting brain maps were aligned to a common space across volunteers. Load pressure and MRI signal magnitudes were positively correlated across all tissue types. These relationships followed brain tissue boundaries (Figure 5A), and were slightly more pronounced in gray matter than in other tissue types (Figures 3A–3D). The relationship between load pressure and Valsalva valley magnitudes was slightly weaker, with principally negative slopes across all tissue types, strongest in CSF, and also followed tissue boundaries (Figure 5B). Region-of-interest calculations showed that valley magnitude and load pressure slopes were larger in gray matter than in white matter (Figures 3E–3H).

Spatial Similarity of Signal Changes Across Trial Types

While each image in Figure 4B has the same intensity scaling, Figure 4C uses relative scaling to help compare the image contrast across scan times. These relative spatial maps of magnitudes across tissue types are difficult to visually distinguish across trial types whether from breath holding, a 20-second Valsalva maneuver, or a 5-second increase in chest pressure.

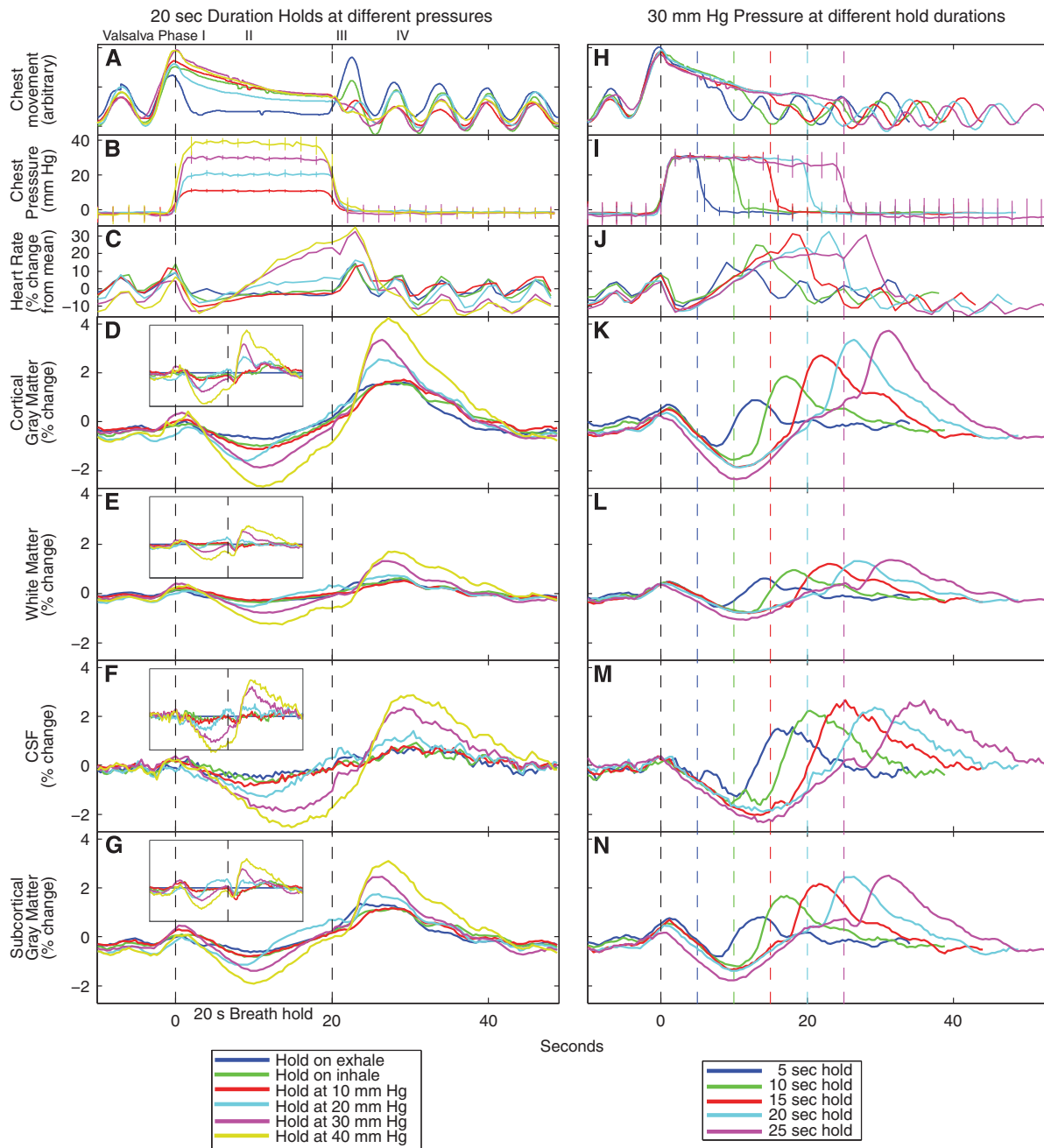


Figure 2. Group averaged responses during Valsalva and breath hold challenges. (A–G) Responses when the breath hold duration is always 20 seconds, but intrathoracic pressure is changing. The vertical dashed lines show the onset and offset of the hold, and the inset shows the signals after the breath hold after the exhalation response is subtracted from the other responses. The inset boxes are proportionally scaled from the larger figures. (H–N) Responses when intrathoracic pressure is always 30 mm Hg, but the breath hold duration is changing. The black dashed line is the onset of the breath hold, and the colored dashed lines mark the end of each breath hold duration. In all regions of interest, the magnetic resonance imaging (MRI) responses decreased below baseline (the valley) during the hold, and increased to a peak after the end of the hold. The magnitude of the responses scaled with thoracic pressure. CSF, cerebrospinal fluid.

To quantify this intrasubject relationship across the population, linear regressions were calculated across gray-matter voxels for each pair of conditions within each subject’s gray-matter voxels. Voxels in gray-matter masks that showed more than a 30% signal change were assumed to be artifacts, and excluded (0.5% to 3% of voxels per subject). Figure 6A shows a scatter plot and the linear fit of breath hold-after-exhalation versus a 5-second breath hold at 30 mm Hg from the subject with the lowest R^2 for this condition.

The r values for the fit qualities were Fisher Z-transformed, and the bar plots in Figure 6B show the peak and valley magnitude relationships between the breath hold on exhalation trials versus all other trials. The voxelwise linear regressions of the peak and valley magnitudes between all pairs of trial types were significant ($P \ll 0.001$). These data show that the relative response magnitudes across gray matter are similar across different thoracic pressure and breath hold durations. This means that the MRI signal changes

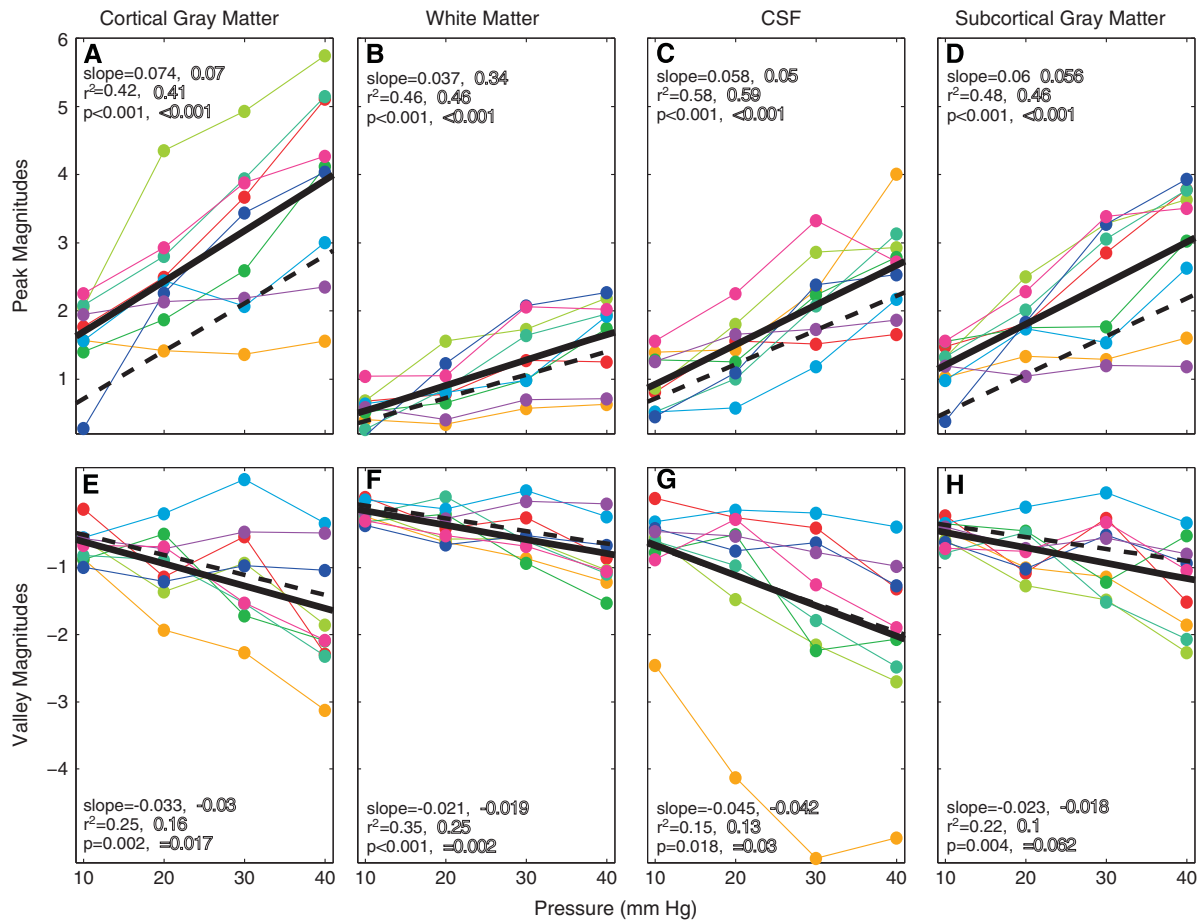


Figure 3. Peak (A–D) and valley (E–H) magnetic resonance imaging (MRI) signal amplitudes, scaled with Valsalva pressure in all brain tissues. Each colored line represents data from a single subject. The solid black lines show the linear regression fits of these data across subjects. To characterize the effect of hypercapnia versus load pressure, the breath hold ending on exhalation response was subtracted from the 10 to 40 mm Hg responses. The dashed lines show the linear regression fits after the breath holds-on-exhalation responses were subtracted. The slope, r^2 , and P -values for each regression are shown in solid lettering for the original data, and in outline lettering after subtracting the breath hold on exhalation. CSF, cerebrospinal fluid.

	5 seconds	10 seconds	15 seconds	20 seconds	25 seconds
Time-to-peak	8.6 ± 0.9	7.6 ± 1.0	7.7 ± 1.2	7.4 ± 1.2	6.9 ± 1.0
Time-to-valley	8.3 ± 1.2	11.7 ± 1.2	11.9 ± 1.6	10.8 ± 1.8	10.5 ± 1.6

Time-to-peak and time-to-valley in seconds for different duration breath holds with a 30 mm Hg target intrathoracic pressure. To normalize for different duration breath holds, time-to-peaks are the time from the end of each breath hold, while time-to-valleys are from the start of each breath hold. Values are mean ± standard deviation values across subjects for voxels within the cortical gray-matter ROI.

caused by having subjects to hold their breath for 20 seconds can be significantly modeled by having them instead increase chest pressure for only 5 seconds.

DISCUSSION

We showed that it is possible to parametrically alter the magnitude of the fMRI BOLD weighted by changing intrathoracic pressure. By keeping the breath hold duration constant while modulating pressure, we showed that the pressure changes alter the BOLD-weighted response independently from hypercapnia-

based changes. The Valsalva had a bimodal response, with an initial dip in signal magnitude at the outset of the challenge, followed by a rise above baseline after the breath hold release. When intrathoracic pressure increased, the magnitude of the valley during the breath hold linearly decreased, and the peak magnitude response linearly increased (Figures 2, 3 and 5). The relative response magnitudes across voxels matched tissue boundaries, and revealed a similar pattern for multiple intrathoracic pressures and breath hold durations (Figures 4 and 6).

Origins of the Valsalva Magnetic Resonance Imaging Response

While the precise origins of the Valsalva-induced MRI response are unclear, aspects of the response suggest a predominantly hemodynamic effect. Increases in intrathoracic load pressure caused both increased heart rate and MRI response magnitudes. The timing of the heart rate minima and maxima during the Valsalva maneuver matched minimal and maximal MRI signals, suggesting that autonomic responses during the Valsalva action are closely coupled to these global changes; CBF changes are known to correlate with arterial blood pressure changes throughout the Valsalva maneuver.^{6,8} Functional MRI signal responses to the Valsalva maneuver varied across tissue types, with gray-matter regions showing greater responsiveness than white matter, but

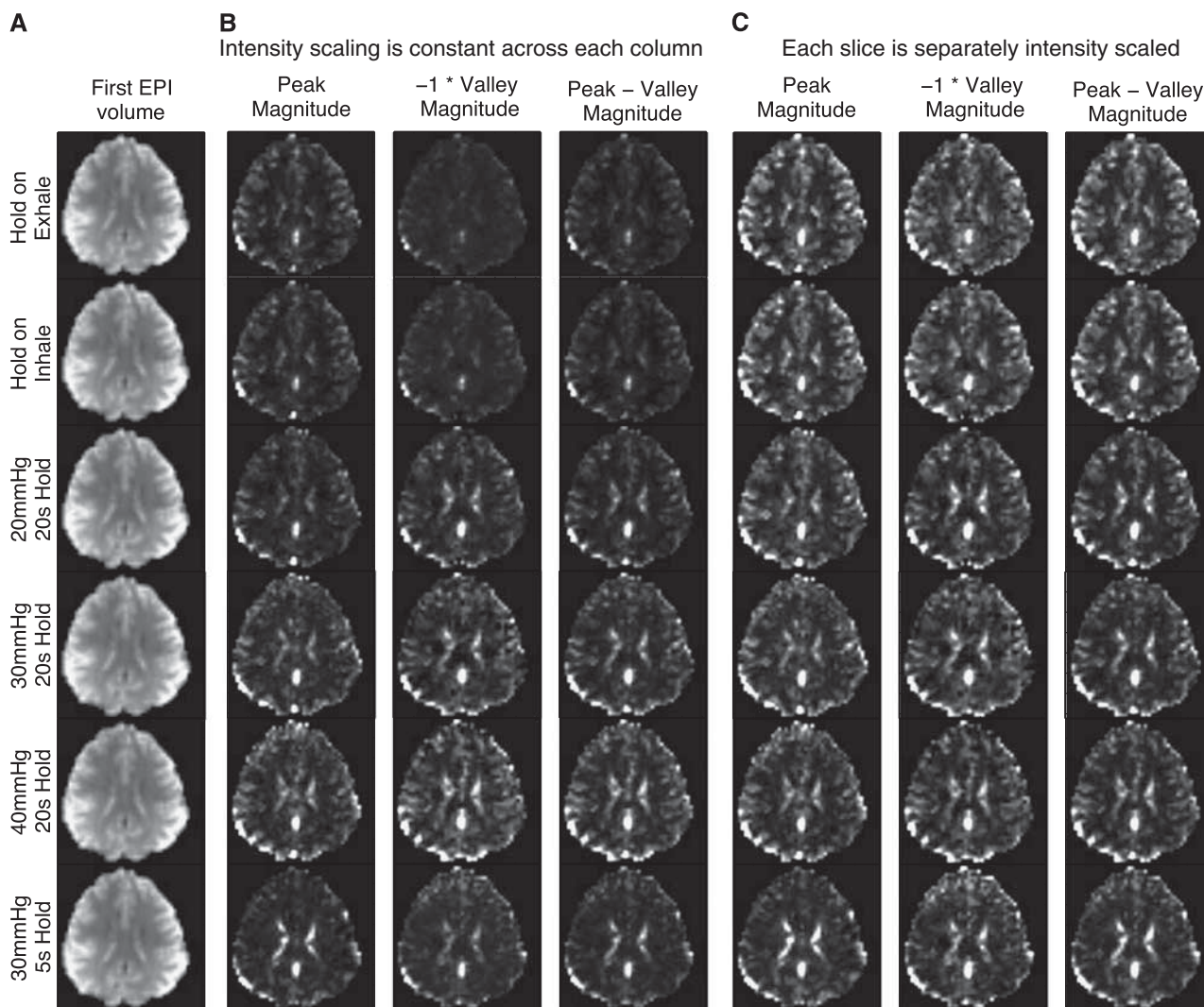


Figure 4. Comparison of magnetic resonance imaging (MRI) signal magnitudes during breath holding and Valsalva conditions. The intensity scale of runs from 2% (black) to 98% (white) of the cumulative distribution of the magnitudes. **(A)** The first EPI volume of each run. **(B)** The intensity scale is constant across each column. The raw magnitudes change within trial type, but the relative tissue contrast remains similar. **(C)** The intensity scale is calculated separately for each slice. The maps of peak magnitude, $-1 \times$ valley magnitude, and the difference between peak and valley magnitudes appears similar across breath hold and Valsalva conditions, even when the Valsalva maneuver duration is only 5 seconds.

equivalent timing. Hypercapnia also induces a greater MRI signal increase in gray over white matter,^{14–18} as does hypoxia.¹⁹

The fMRI temporal response pattern for all Valsalva challenges closely resembles the known Valsalva Transcranial Doppler cerebral blood flow velocity response in timing and shape,^{7,8} with the fMRI signal and cerebral blood flow velocity both decreasing and reaching a minima during the load period, followed by an overshoot upon release, and a return to baseline. During the initial decline, decreased CBF^{7,8} could lead to reduced venous return and blood volume, leading to increased oxygen extraction, reduced venous $[O_2]$, and reduced $[O_2]$ blood concentration, causing a decrease in signal. Upon release, the increase in CBF may result in an enrichment in oxyhemoglobin, leading to a rise in signal intensity.

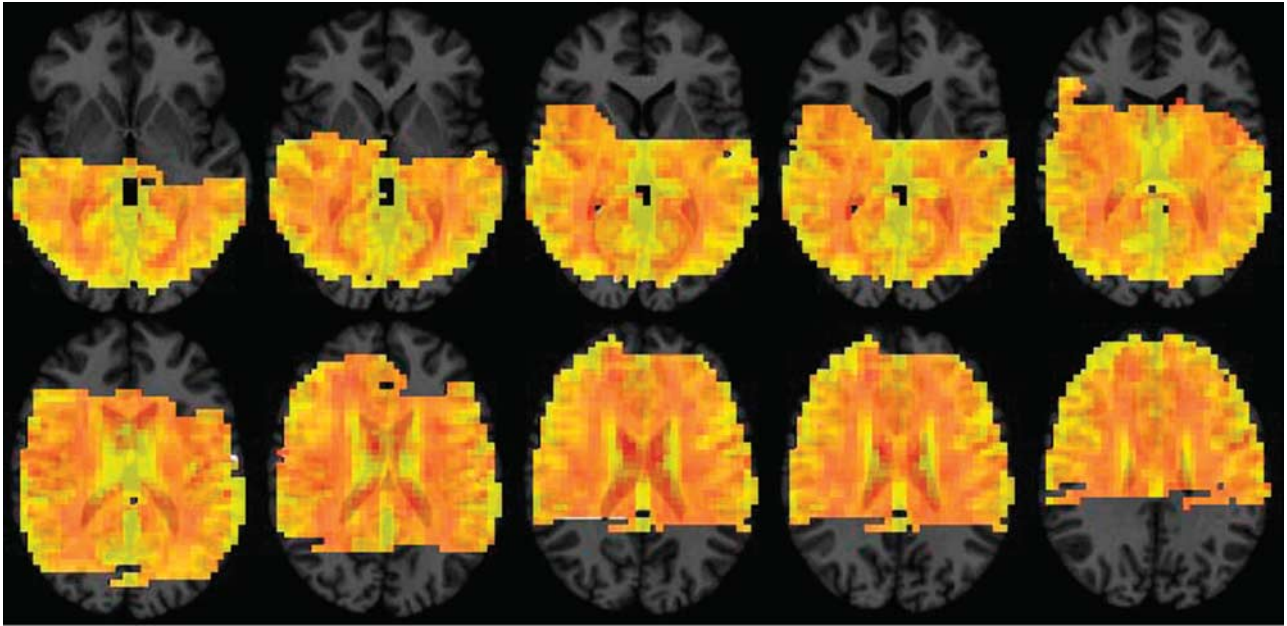
Even though both the heart rate and fMRI responses increased with increased intrathoracic pressure, we found no consistent linear time-invariant transfer function linking the two responses across all task conditions. This is partially because heart rate alone does not define blood flow and deoxyhemoglobin concentration during a Valsalva maneuver. For example, neither well-known

cardiac stroke volume changes during the Valsalva maneuver nor total blood oxygenation changes during a breath hold would be modeled by heart rate.

Functional MRI signal changes also appeared in CSF during the Valsalva maneuver; CSF pressure effects are unlikely to contribute to these changes since CSF pressure reaches, and remains relatively constant at, or above the Valsalva pressure throughout the hold, an outcome that does not match the bimodal MRI signal response.^{20,21} Partial volume effects from the tissue surrounding CSF may contribute, but all voxels that contained 25% or more than one tissue type were removed from analysis. Some signal change might result from the vasculature in the choroid plexus showing BOLD changes, or from slowed venous return, a consequence of increased intrathoracic pressure, leading to increased cerebral blood volume. Such a process could cause an intrathoracic pressure-modulated initial decrease in the Valsalva response in all tissues and choroid plexus. Another mechanism for the CSF-related signal changes is that the Valsalva-induced reduced CSF flow may increase radio frequency saturation, causing a signal decrease, due to incomplete longitudinal relaxation.

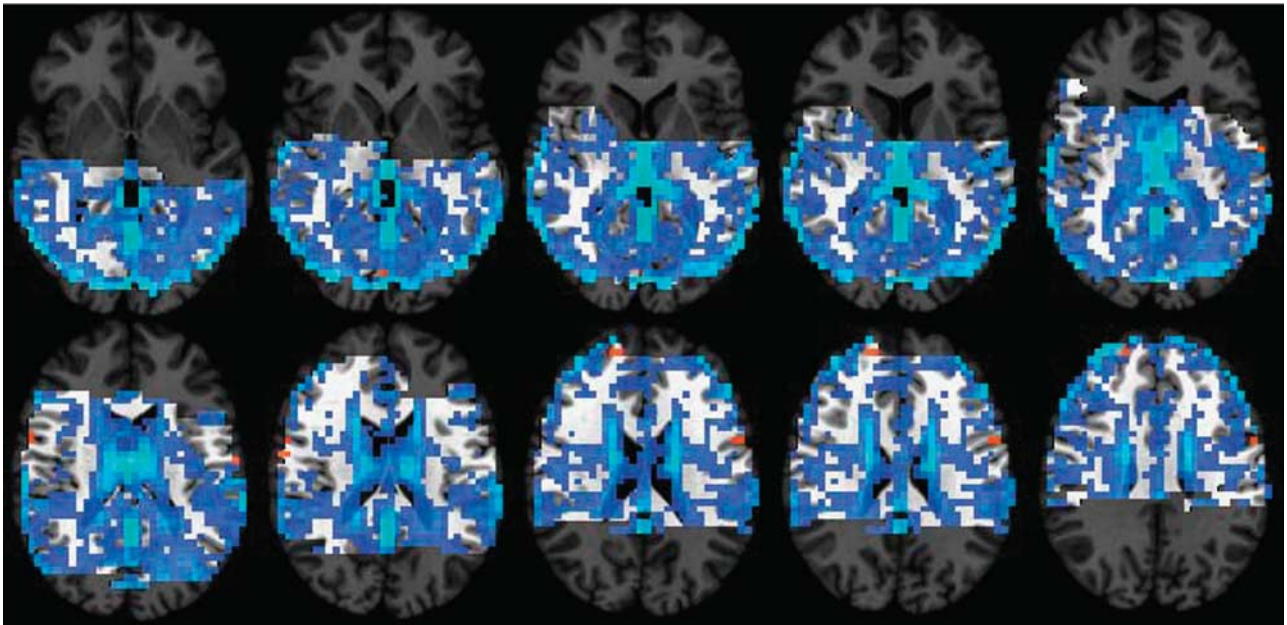
A

Group Averaged Slope of Peak Magnitudes vs Chest Pressure



B

Group Averaged Slope of Valley Magnitudes vs Chest Pressure



Slope (% change from 10-40 mm Hg)

-0.9% 0.9%

Figure 5. Slope of pressure versus (A) peak or (B) valley magnetic resonance imaging (MRI) signal responses. Slopes were calculated for each voxel in the same manner as in Figure 3. The data are thresholded to exclude slopes of less than 0.15%. The anatomic underlay is darkened for voxels with no fMRI data. The slopes were steeper in gray matter than in white matter.

Potential of Valsalva-Based Tasks for Functional Magnetic Resonance Imaging Calibration and for Cerebrovascular and Autonomic Assessment

The BOLD-weighted functional MRI signal is most commonly used as an indirect measure of neural activity. However, nonneural vascular factors, such as cerebral blood flow, hematocrit, resting cerebral blood volume, and the size and location of veins vary

among brain regions, subjects, and disease conditions, and can hamper accurate detection of that neural activity.¹

Hypercapnic challenges induce global cerebral blood flow global changes. By causing the BOLD-weighted signal to change in a well-understood manner, such tests, including the breath hold, are useful in calibrating fMRI signals, and have been used to characterize nonneuronal hemodynamic factors, such as the

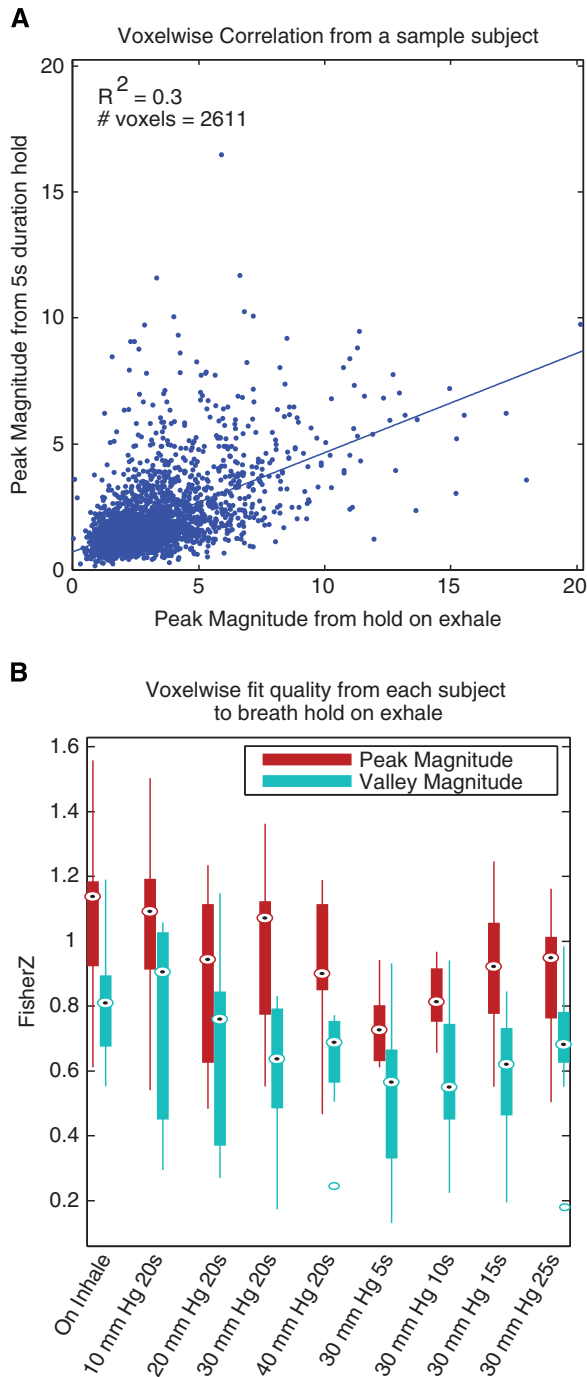


Figure 6. Voxewise relationships between trials. **(A)** The relationship between the peak magnitudes for a 20-second breath hold on exhalation (no pressure target) versus a 5-second hold at 30 mm Hg. The subject with the lowest r^2 value for this fit is shown. Each point represents a gray-matter voxel. The linear fit to all voxelwise data is shown. **(B)** For each trial, compared with breath hold on exhalation, the r values from the regressions shown in **(A)** were Fisher Z-transformed and averaged across subjects. Box plots show the median (circle with dot), 25th and 75th percentiles (solid box), maxima and minima (whiskers) and outliers (hollow circles). Every fit is significant.

distribution of baseline venous blood volume, so that magnitude changes from neural factors can be more accurately measured.^{1–3,22–25} The Valsalva maneuver induces global effects similar in pattern to those induced by hypercapnia and other

global flow change stressors. A 5-second increase in intrathoracic pressure produces a similar response to a 20-second breath hold. Designing a breath holding study to maintain consistent intrathoracic pressure may increase precision,^{9,10} and the ability to use measured variation of intrathoracic pressure to modulate response magnitudes may allow for more accurate cerebrovascular measurements.

For situations where researchers want to use a standard breath hold, the findings here show an important contrast between initiating a breath hold after exhalation or inhalation. Thomason *et al*⁹ conducted breath holds after a final inhalation, and used chest circumference as an indirect measure of intrathoracic pressure. They hypothesized that a breath hold after inhalation includes a Valsalva effect from pressure increases, even when volunteers do not consciously attempt to increase intrathoracic pressure.⁹ We found that the response to breath hold after inhalation is similar to maintaining a 10 mm Hg pressure (Figure 2), which supports their findings. Studies that use hypercapnic challenges alone without measurements of intrathoracic pressure could unwittingly introduce uncontrolled pressure-related effects in their experimental results. The Valsalva, with its constant pressure feedback, therefore offers a more precise assessment for any hypercapnic challenge.

We also showed that a breath hold after exhalation has notable time course differences from a breath hold after inhalation; the signal undershoot during the breath hold is much lower, while the signal increase after the hold is similar to the breath hold after exhalation and with 10 mm Hg of pressure (Figures 2 and 3). These data imply that the initial BOLD undershoot is due more to pressure changes than hypercapnia, and the peak after the hold results more from hypercapnia. If one does not measure intrathoracic pressure, then breath holding after exhalation is a more direct measure of hypercapnia, with one less potential source of response variation than holding after inhalation.

These interstudy and interparadigm variations make direct comparisons across subjects and studies difficult to interpret without a more directly unifying means of quantifying compliance and task performance. Our basic Valsalva apparatus involved exhaling into a single plastic tube connected to a very simple pressure transducer located outside the scan room, but provided verification of subject compliance and performance, and controlled for thoracic pressure effects noted above. It may also be possible to assess end tidal CO₂ content after each breath hold as a proxy for the amount of hypercapnia. As opposed to trusting that a patient is holding their breath the entire time, and holding it with or without pressure, the Valsalva apparatus allows the researcher to measure an additional source of known variation.

CONCLUSION

This study examined BOLD-weighted MRI responses to multiple parametrically varied pressures and durations of the Valsalva maneuver in a single setting. We show that performing the maneuver at varied pressures modulates the MRI signal amplitude and heart rate response. The MRI signal change maps, obtained in the first 15 seconds of the procedure, closely resemble those obtained using other global flow change stressors. While our study did not directly test calibration, these findings may potentially lead to a calibration tool or cerebral autoregulation assessment with improved precision, simplicity, noninvasiveness, and subject tolerance, compared with existing methods. The physiologic mechanisms underlying these signal changes need to be explored more fully.

DISCLOSURE/CONFLICT OF INTEREST

The authors declare no conflict of interest.

ACKNOWLEDGMENTS

The authors thank George Dold and Thomas Talbot for assistance with development of pressure recording and stimulus presentation software and hardware setup, Hang Joon Jo for assistance with Freesurfer segmentations, and Catie Chang for feedback in several areas including on the relationship between our heart rate changes and fMRI responses.

REFERENCES

- 1 Bandettini PA, Wong EC. A hypercapnia-based normalization method for improved spatial localization of human brain activation with fMRI. *NMR Biomed* 1997; **10**: 197–203.
- 2 Davis T, Kwong K, Weisskoff R, Rosen B. Calibrated functional MRI: mapping the dynamics of oxidative metabolism. *Proc Natl Acad Sci USA* 1998; **95**: 1834.
- 3 Hoge RD, Atkinson J, Gill B, Crelier GR, Marrett S, Pike GB. Linear coupling between cerebral blood flow and oxygen consumption in activated human cortex. *Proc Natl Acad Sci USA* 1999; **96**: 9403–9408.
- 4 Blockley NP, Griffeth VEM, Simon AB, Buxton RB. A review of calibrated blood oxygenation level-dependent (BOLD) methods for the measurement of task-induced changes in brain oxygen metabolism. *NMR Biomed* 2013; **26**: 987–1003.
- 5 Elisberg EI. Heart rate response to the valsalva maneuver as a test of circulatory integrity. *JAMA* 1963; **186**: 200.
- 6 Greenfield JC, Rembert JC, Tindall GT. Transient changes in cerebral vascular resistance during the Valsalva maneuver in man. *Stroke* 1984; **15**: 76–79.
- 7 Tiecks FP, Lam AM, Matta BF, Strebel S, Douville C, Newell DW. Effects of the valsalva maneuver on cerebral circulation in healthy adults. A transcranial Doppler Study. *Stroke* 1995; **26**: 1386–1392.
- 8 Dawson SL, Panerai RB, Potter JF. Critical closing pressure explains cerebral hemodynamics during the Valsalva maneuver. *J Appl Physiol* 1999; **86**: 675–680.
- 9 Thomason ME, Glover GH. Controlled inspiration depth reduces variance in breath-holding-induced BOLD signal. *NeuroImage* 2008; **39**: 206–214.
- 10 van Beek AH, de Wit HM, Olde Rikkert MG, Claassen JA. Incorrect performance of the breath hold method in the old underestimates cerebrovascular reactivity and goes unnoticed without concomitant blood pressure and end-tidal CO₂ Registration. *J Neuroimaging* 2011; **21**: 340–347.
- 11 Cox RW. AFNI: Software for analysis and visualization of functional magnetic resonance neuroimages. *Comput Biomed Res* 1996; **29**: 162–173.
- 12 Fischl B, Dale AM. Measuring the thickness of the human cerebral cortex from magnetic resonance images. *Proc Natl Acad Sci USA* 2000; **97**: 11050–11055.
- 13 Murray WB, Foster PA. The peripheral pulse wave: information overlooked. *J Clin Monit Comput* 1996; **12**: 365–377.
- 14 Kastrup A, Kruger G, Glover G, Neumann-Haefelin T, Moseley M. Regional variability of cerebral blood oxygenation response to hypercapnia. *NeuroImage* 1999; **10**: 675–681.
- 15 Kwong K, Wanke I, Donahue K, Davis T, Rosen B. EPI imaging of global increase of brain MR signal with breath-hold preceded by breathing O₂. *Magn Reson Med* 1995; **33**: 448–452.
- 16 Li T, Kastrup A, Takahashi A, Moseley M. Functional MRI of human brain during breath holding by BOLD and FAIR techniques. *NeuroImage* 1999; **9**: 243–249.
- 17 Stillman A, Hu X, Jerosch-Herold M. Functional MRI of brain during breath holding at 4T. *Magn Reson Imaging* 1995; **13**: 893–897.
- 18 Rostrup E, Larsson HB, Toft PB, Garde K, Ring PB, Henriksen O. Susceptibility contrast imaging of CO₂-induced changes in the blood volume of the human brain. *Acta Radiol* 1996; **37**: 813–822.
- 19 Stehling MK, Schmitt F, Ladebeck R. Echo-planar MR imaging of human brain oxygenation changes. *J Magn Reson Imaging* 1993; **3**: 471–474.
- 20 Greenberg J, Alavi A, Reivich M, Kuhl D. Local cerebral blood volume response to carbon dioxide in man. *Circulation Research* 1978; **43**: 324–331.
- 21 Hamilton W, Woodbury R, Harper H. Arterial, cerebrospinal and venous pressures in man during cough and strain. *Am J Physiol* 1944; **141**: 0042–0050.
- 22 Handwerker DA, Gazzaley A, Inglis BA, D'Esposito M. Reducing vascular variability of fMRI data across aging populations using a breathholding task. *Hum Brain Mapp* 2007; **28**: 846–859.
- 23 Thomason M, Foland L, Glover G. Calibration of BOLD fMRI using breath holding reduces group variance during a cognitive task. *Hum Brain Mapp* 2007; **28**: 59–68.
- 24 Cohen E, Rostrup E, Sidaros K, Lund T, Paulson O, Ugurbil K et al. Hypercapnic normalization of BOLD fMRI: comparison across field strengths and pulse sequences. *NeuroImage* 2004; **23**: 613–624.
- 25 Hyder F. Neuroimaging with calibrated. *fMRI* 2004; **35**: 2635–2641.
- 26 Macey PM, Wu P, Kumar R, Ogren JA, Richardson HL, Woo MA et al. Differential responses of the insular cortex gyri to autonomic challenges. *Auton Neurosci* 2012; **168**: 72–81.